Earth and Planetary Science Letters 450 (2016) 186–196

Contents lists available at ScienceDirect

Earth and Planetary Science Letters

www.elsevier.com/locate/epsl

# High-resolution Holocene South American monsoon history recorded by a speleothem from Botuverá Cave, Brazil

J.P. Bernal [a,*], Francisco W. Cruz [b], Nicolás M. Stríkis [b,c], Xianfeng Wang [d], Michael Deininger [e], Maria Carolina A. Catunda [b], C. Ortega-Obregón [a], Hai Cheng [f,g], R. Lawrence Edwards [g], Augusto S. Auler [h]

[a] Centro de Geociencias, Universidad Nacional Autónoma de México, Campus UNAM, Juriquilla, Querétaro 76230, México
[b] Instituto de Geociências, Universidade de São Paulo, Rua do Lago 562, Sao Paolo, Brazil
[c] Departamento de Geoquímica, Universidade Federal Fluminense, Rua Outeiro de São João Batista, s/n, Niterói, Brazil
[d] Earth Observatory of Singapore, Nanyang Technological University, Singapore
[e] School of Geological Sciences, University College Dublin, Belfield, Dublin 4, Ireland
[f] Institute of Global Environmental Change, Xi'an Jiaotong University, Xi'an, China
[g] Department of Geology and Geophysics, University of Minnesota, Minneapolis, MN 55455, USA
[h] Instituto do Carste, Rua Brasópolis, 139, Floresta, Belo Horizonte, MG, Brazil

ARTICLE INFO

*Article history:*
Received 10 December 2015
Received in revised form 1 June 2016
Accepted 4 June 2016
Available online 5 July 2016
Editor: H. Stoll

*Keywords:*
Holocene
Brazil
stalagmite
trace-elements
SAMS/SACZ

ABSTRACT

A Holocene stalagmite from Botuverá Cave, southeastern Brazil was analyzed by LA-ICPMS for Mg/Ca, Sr/Ca, Ba/Ca. The observed variability in the record was demonstrated to be modulated by prior calcite precipitation, and, thus, is interpreted to reflect monsoon intensity. We find that the calcite $\delta^{18}O$ is strongly correlated with Sr/Ca, indicating that atmospheric circulation over South America and monsoon intensity have been tightly correlated throughout most of the Holocene, both directly responding to solar precession. Comparison with other contemporaneous high-resolution hydroclimate records reveals that SAMS has shown a degree of complexity during the Holocene not previously detected, with periods where the South American Convergence Zone (SACZ) expanded to cover most of the South American subcontinent, and coincident with periods of low-SST in the north Atlantic. We also detect periods where rainfall amount in northeastern and southeastern Brazil are markedly anti-phased, suggesting a north-south migration of SACZ, which it appears to be mediated by solar irradiance. The high-resolution nature of our record allow us to examine the effect that Holocene climate anomalies had upon SAMS dynamics and hydroclimate in southeastern Brazil, in particular the 8.2 ka event and the Little Ice Age. In addition to confirm the internal structure of the events, we also detect the possible consequences of the climatic anomalies upon ocean–atmosphere interactions through its effects upon SAMS.



## 1. Introduction

The South American Monsoon System (SAMS) refers to the austral summer season features of deep convective activity and large scale circulation over South America (Liebmann and Mechoso, 2011) from which one of most important biodiversity hotspot in the tropics, the Atlantic Rainforest, has relied upon during late Quaternary (Carnaval et al., 2009), and it is the main source of rainfall for the most densely-populated areas of South America. Because of its importance, an increasing number of studies have focused on deciphering the natural variability of SAMS on orbital to millennial time-scales and have established links to Northern Hemisphere climate (e.g. Cruz et al., 2005a, 2009; Stríkis et al., 2011; Wang et al., 2006). More recently, high-resolution paleoclimate records from South America have been able to reveal the modulation/coupling of SAMS by different (multi)decadal climatic modes, and/or solar oscillations (Apaéstegui et al., 2014a; Bird et al., 2011; Chiessi et al., 2009; Novello et al., 2012; Thompson et al., 2013; Vuille et al., 2012). Most of these reconstructions are focused on the last two millennia, and only Chiessi et al. (2009) cover a period of ~4.5 ka during the last glacial maximum; yet, there is still no reconstruction of SAMS in subtropical South America providing evidence for hydroclimate modulation by multi-decadal climatic modes during the entire Holocene period when climate changed substantially from low to high phases of austral summer insolation. In this regard, it is necessary to obtain long, well-dated and

* Corresponding author.
*E-mail address:* jpbernal@unam.mx (J.P. Bernal).

http://dx.doi.org/10.1016/j.epsl.2016.06.008
0012-821X/

highly resolved records of past SAMS's activity in an attempt to discuss the possible modulation of precession forcing on the high frequency precipitation variability. Such records also have the potential to provide valuable information on the coupling/decoupling of monsoonal systems with the different climatic modes, and/or reveal the possible influence from solar activity on climate instability or abrupt climate changes, providing a unique insight into the high-resolution paleoclimate dynamics during such events.

Oxygen-isotope records from stalagmites have provided many robust paleoclimate reconstructions spanning several thousands of years because variability in the carbonate $\delta^{18}O$ can be interpreted to reflect changes in the isotopic composition of local rainfall, which can be a function of moisture source, rainfall amount, or atmospheric equilibrium temperature (Lachniet, 2009). However, obtaining $\delta^{18}O$ records with high temporal resolution is complex and labor intensive (e.g. Treble et al., 2007), and is usually limited to samples with relatively high growth rates (>50 μm/yr), hampering our general understanding on how high-frequency climate modes and solar oscillations might have potentially impacted the different monsoonal systems in the world. This has led to the development of alternative rainfall proxies in stalagmites, among which, trace element variability is probably the most promising (Fairchild and Treble, 2009).

Trace element variability in stalagmites has been studied for several years (Fairchild and Treble, 2009), but the complexity and variety of geochemical processes to which they can be subjected in the epikarst hampers the establishment of a general model to explain trace element variations. Yet, the increasing knowledge on the geochemical processes modulating the abundance of some trace elements in the epikarst, as well as their incorporation into the speleothem calcite (Sinclair, 2011; Stoll et al., 2012; e.g. Treble et al., 2005; Tremaine and Froelich, 2013), along with the development and availability of different microbeam techniques, have permitted the construction of records with high spatial- and chronological resolution using laser ablation-ICPMS (Treble et al., 2003), secondary ionization mass-spectrometry (Smith et al., 2009) and micro-XRF (e.g. Borsato et al., 2007); thus allowing the construction of records with high-temporal resolution even from slow-growing stalagmites, which can complement complex $\delta^{18}O$ records.

Long trace element records can also provide additional information for the interpretation of speleothem $\delta^{18}O$ records where the isotopic composition of local precipitation and seepage, which is finally recorded by speleothems, can be modulated by more than one fractionation process (e.g. source and rainfall amount). This is the case of southern Brazil, where two isotopically distinct moisture sources, Amazonian and extratropical, dominate rainfall regimes during the summer and winter, respectively (Cruz et al., 2005a). Consequently, speleothem $\delta^{18}O$ cannot be used as a proxy of mean rainfall accumulation because the amount effect is not evident and is poorly correlated with $\delta^{18}O$ in the region (Cruz et al., 2005b; Vuille and Werner, 2005). If, however, the variability on the abundance of trace elements is demonstrated to be modulated by karst humidity and prior calcite precipitation, such as in caves from Southeastern Brazil (Karmann et al., 2007), then it is possible to build a more complete and precise hydroclimate reconstruction. Indeed, by examining the variability of both, trace element and $\delta^{18}O$ records, it can be possible to obtain information on changes in moisture sources and amount with high temporal resolution, providing a more detailed description of the climatic patterns and atmosphere dynamics modulating hydroclimate in the area.

Here, we present a high-resolution trace element record in a stalagmite from Botuverá Cave (southeastern Brazil) spanning most of the Holocene using LA-ICP-MS providing the most detailed record of Holocene hydroclimate yet available for this area. Paleoclimate records from this cave are, arguably, among the most robust climate reconstructions for South America (Cruz et al., 2006a, 2005b; Wang et al., 2006, 2007), but due to the slow growth rate exhibited by the collected stalagmites (2–10 μm/yr), construction of records of hydroclimate variability based on calcite $\delta^{18}O$ with high temporal-resolution is difficult. We present evidence supporting that the observed variability in trace elements is mostly modulated by changes in the karst humidity, thus rainfall amount. This allows us to identify the diverse set of climatic modes (e.g. AMO) and forcing mechanisms (e.g. solar variability) that have been modulating the strength of the South American Monsoon System, and determine that SAMS evolution throughout the Holocene has been the result from a complex interplay by different forcing mechanisms.

## 2. Samples and methods

Botuverá cave (Fig. 1, 27°13′S; 49°09′W, 230 m above sea level) is located in Santa Catarina State, Southern Brazil, and is hosted within carbonates and sediments from the Brusque Group (Auler, 2002), a succession of metavolcanosedimentary rocks from the Neoproterozoic with an age of c.a. 600 Ma (Basei et al., 2011). Sample BTV21a is a 22.5 cm long stalagmite collected in 2002. Visual inspection of the sample reveals that there are no evident changes in growth direction or long hiatuses, an observation supported also on the resulting age-model (Fig. 2). Modern climatic conditions in the area have been described elsewhere (Cruz et al., 2007). The stalagmite was sectioned and a linear age-model was developed from 13 U/Th ages measured at the Minnesota Isotope Laboratory, University of Minnesota, and at the Earth Observatory of Singapore, using the methods described in Shen et al. (2002).

Oxygen and carbon stable isotope analyses were carried out at the University of Minnesota following the procedures and quality control described in Wang et al. (2006). Trace element ratios were obtained by Laser-ablation ICP-MS using a Resonetics L-50 excimer laser-ablation workstation (ArF, $\lambda = 193$ ns, 23 ns FWHM, fluence of ~6 J/cm$^2$) at Centro de Geociencias, Universidad Nacional Autónoma de México (UNAM). Details on the analytical protocols used here are described in the supplemental material.

Spectral analyses were carried out on sub-annually interpolated time-series using the Redfit module (Schulz and Mudelsee, 2002) as incorporated in PAST v 3.03 (Hammer et al., 2001). Wavelet analysis was performed using a Morlet wavefunction using the protocols developed by Grinsted et al. (2004) for Matlab®.

## 3. Results

### 3.1. Chronology

Stalagmite BTV21a has approximately 90 ng/g of U and only ~0.05 ng/g of Th, thus the average ($^{232}Th/^{238}U$) is 0.00018.[1] Ages were corrected for contributions from detrital material using a two-point isochron, assuming that the detrital material present in the stalagmite has a typical crustal $^{230}Th/^{232}Th = (4.4 \pm 2.2) \times 10^{-6}$ and $(^{232}Th/^{238}U) = 1.2 \pm 0.5$ (McDonough and Sun, 1995) and, essentially, in secular equilibrium; i.e. ($^{230}Th/^{238}U$) and ($^{234}U/^{238}U$) = 1.0 ± 0.1. Nevertheless, because of the very low Th concentration in the stalagmite, the difference between "corrected" and "raw" age is less than 5 yr, with the exception of the two uppermost samples, whose corrected age are 27.5 and 92 yr younger than the uncorrected age. All ages are in stratigraphic order (Fig. 2A, Table SP1) and show that the

[1] Round brackets denote activity ratios calculated using the decay constants from Cheng et al. (2000). We note that using the more recent values reported by Cheng et al. (2013a) does not yield significantly different activity ratios, ages or uncertainties.

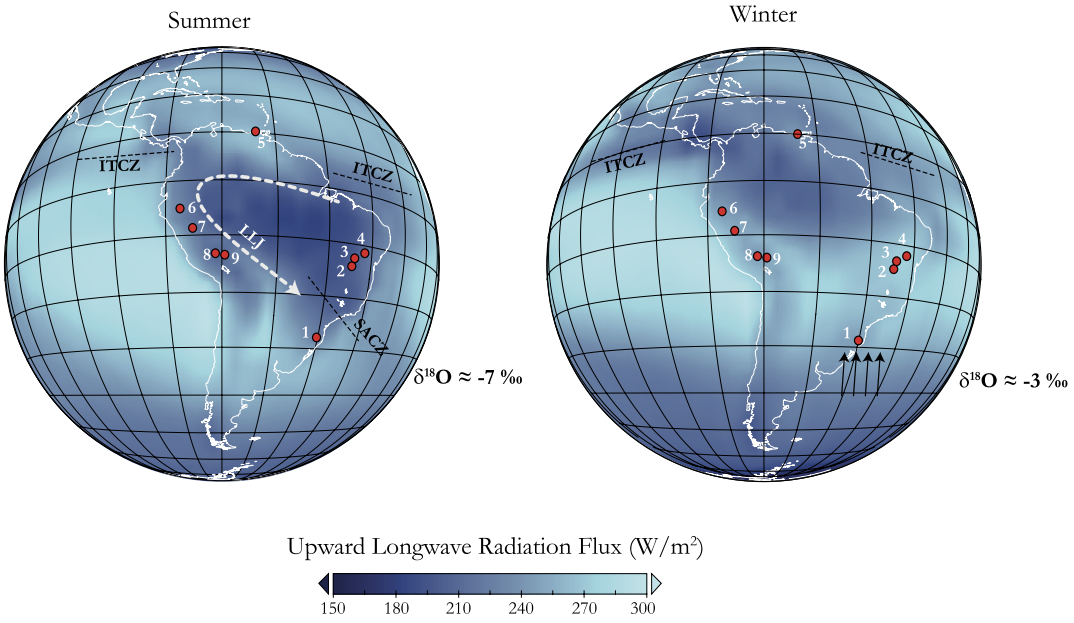


**Fig. 1.** Summer and winter 1950–2010 average upward longwave radiation flux as an indicator of convective activity over South America (data from NCEP Reanalysis 2 data provided by the NOAA/OAR/ESRL PSD, Boulder, Colorado, USA, from their Web site at http://www.esrl.noaa.gov/psd/cgi-bin/data/composites/printpage.pl) and highlighting the mean position of the Intertropical Convergence Zone (ITCZ) and the South American Convergence Zone (SACZ). Numbers indicate location of different sites discussed in the text. 1) Botuverá Cave, 2) Lapa Grande cave (Strikis et al., 2011), 3) Padre cave (Cheng et al., 2009), 4) Diva de Maura cave (Novello et al., 2012), 5) Cariaco basin (Haug et al., 2001), 6) Palestina Cave (Apaéstegui et al., 2014b), 7) Huagapo cave (Kanner et al., 2013), 8) Quelccaya glacier (Thompson et al., 2013). White arrow for the summer indicates the general simplified trajectory of the Low Level Jet (LLJ) during summer. Black arrows indicate the simplified trajectory of extratropical moisture. The $\delta^{18}O$ values represent the modern amount weighted average isotopic composition of rainfall at the nearest GNIP station in Porto Alegre, Brazil (Cruz et al., 2005b).

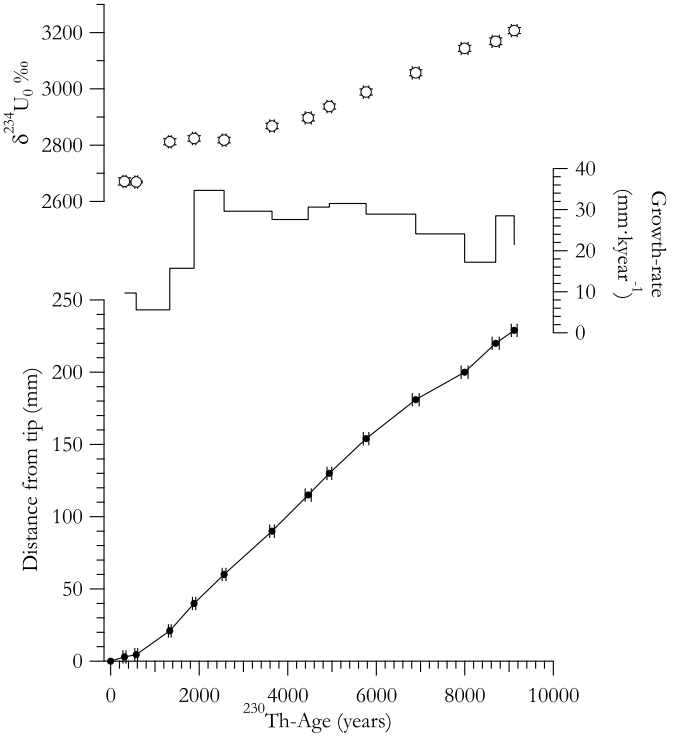


**Fig. 2.** A): $^{230}$Th-ages vs. distance from stalagmite tip to build age-model used in this work. B) growth-rate variability for stalagmite BTV21a, showing that the sample grew ~20–30 μm per year except for the last millennia when growth rate decreased significantly to 10–15 μm per year. C) Initial $\delta^{234}U$ vs. age, showing a gradual decrease from the early to the late Holocene.

sample grew continuously since 9118 ± 17 yr with an average growth rate of 28 ± 4 μm per year with little variability. Growth rate decreased significantly to 17 and 9.5 μm per year between 7000 and 8000 yr B.P. and 1300 to 300 yr B.P., respectively (Fig. 2B). The robustness of the chronology and the age model presented here is supported by the close agreement between our record and other independently-dated records from other localities. Fig. 2C also shows a gradual decrease in $\delta^{234}U_0$ throughout the period of stalagmite growth, from $\delta^{234}U_0 \sim 3200‰$ during the early Holocene to 2680‰ in the late Holocene. The hydrological implications of such shift are discussed below.

### 3.2. Stable isotope

The $\delta^{18}O$ composition of BTV21a varies between −2.1‰ and −4.4‰ (VPDB), and is characterized by a gradual change from less negative, or higher, $\delta^{18}O$ values during the early Holocene to more negative, or lower, $\delta^{18}O$ values during the late Holocene (supplemental material, Fig. SP2), which has been interpreted to reflect increased intensity of SAMS (Cruz et al., 2005a). We note that the $\delta^{18}O$ variability in BTV21a nicely replicates other contemporaneous stalagmites from Botuverá Cave (Cruz et al., 2005a; Wang et al., 2006, 2007), providing strong evidence for calcite precipitation in isotopic equilibrium (supplemental material, Fig. SP2). This is further supported by the absence of any correlation between $\delta^{18}O$ and $\delta^{13}C$ ($R^2 = 0.0303$), which would be expected under isotope kinetic effects (Hendy, 1971). Therefore, kinetic fractionation during calcite precipitation is not a dominant process affecting the $\delta^{18}O$ and $\delta^{13}C$ variability in BTV21a.

### 3.3. Geochemical controls on stalagmite Mg/Ca, Sr/Ca and Ba/Ca

The Mg/Ca, Sr/Ca and Ba/Ca records in BTV21a are composed of nearly fifty-thousand independent points, resulting in a time-series of sub-annual resolution, with an average of five points per year throughout the Holocene. The large variability in the record was reduced by calculating a 200-point running mean using a rectangular window. The “smoothed” time-series are used throughout

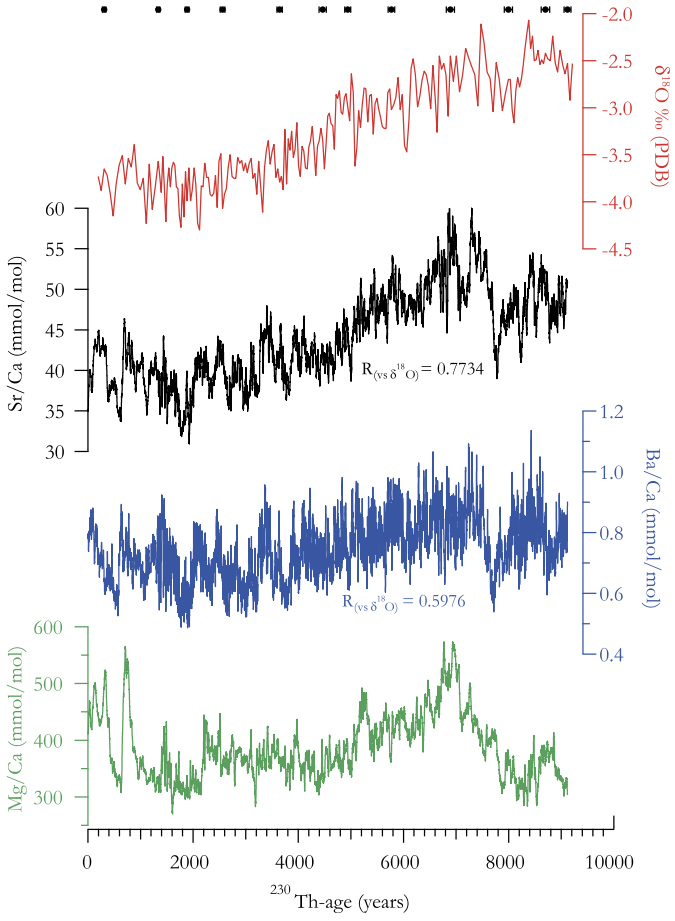


**Fig. 3.** Comparison of hydroclimate proxies from stalagmite BTV21a: from top to bottom: calcite $\delta^{18}O$ (VPDB), Sr/Ca, Ba/Ca and Mg/Ca. Markers at top shows dated parts of the stalagmite.

this work. Despite the high-resolution of the record, no annual cycles were detected in both non-smoothed and smoothed data.

Fig. 3 shows the trace element record for BTV21a. Mg/Ca and Sr/Ca ratios range from 222 to 333 mmol/mol and 60 to 30 mmol/mol, respectively, whilst Ba/Ca ratios vary between 0.5 and 1.1 mmol/mol. In general, the trace element ratios co-vary throughout the Holocene, with exception of the last millennia where two significant and abrupt excursions to high Mg/Ca ratios are observed. A gradual decrease in Mg/Ca, Sr/Ca and Ba/Ca is observed from 7300 yr B.P. onwards.

Several geochemical processes can modulate the relative abundance of trace elements in the stalagmite, such as prior calcite precipitation (PCP), incongruent calcite dissolution (ICD) as well as mixing between two or more sources. From these, only PCP can be linked with external atmospheric conditions, as a lower vadose zone aquifer above the cave favors the precipitation of calcite upstream the stalagmite, as fissure and secondary conduits are ventilated during dry periods, allowing $CO_2$ degasification, thus favoring calcite precipitation and leading to the enrichment of incompatible trace elements, such as Mg, Sr and Ba, relative to Ca in the seepage water, hence, the stalagmite (Fairchild et al., 2000). Conversely, during wet periods, precipitation of calcite upstream the seepage flow pathway is less likely to occur since the karstic porosity where $CO_2$ degasification takes place are likely to be filled with water, resulting in little or no significant change in the relative concentration of trace elements. Consequently, it is essential to identify which, of any of these processes, is more significant in modulating the observed variability in Mg/Ca, Sr/Ca and Ba/Ca.

Sinclair (2011) has demonstrated that if PCP modulates Mg/Ca and Sr/Ca variability, and in the absence of kinetic control, the molar ratios (mol Mg/mol Ca and mol Sr/mol Ca) should co-vary linearly in a ln-space, with a slope of $0.88 \pm 0.13$. Fig. 4A shows that ln(Mg/Ca) and ln(Sr/Ca) from BTV21a have a strong linear covariation ($R = 0.51$), but fail to represent the expected trend if PCP were the only process modulating their variability, as the resulting slope ($m = 0.55$) indicates that other processes, have impinged upon the abundances of Mg and Sr in the stalagmite. This is probably the result from dissolution of high-Mg carbonates from the Brusque group (Basei et al., 2011) where the caves is hosted. In particular Mg/Ca appears to be more affected as it shows large and abrupt variability during the last millennia, not observed in the Sr/Ca record, suggesting the presence of an additional source of Mg but not of Sr to the seepage waters in the karstic environment. This implies that while Mg variability might be affected by two or more geochemical processes in the epikarst, they might not have affected significantly the Sr/Ca variability in the BTV21a trace-element record.

To verify whether Sr/Ca was mostly modulated by PCP, we tested the thermodynamic and kinetic assumptions of Sinclair (2011), using the experimentally derived distribution coefficients for Sr/Ca and Ba/Ca at 25 °C by Day and Henderson (2013). Accordingly, if PCP modulated their variability during stalagmite growth, then the observed molar ratios should co-vary linearly in the ln-space, with a slope of $1.02 \pm 0.08$. Fig. 4B shows that the Sr/Ca and Ba/Ca molar ratios measured in BTV21a closely follows the expected trend, suggesting that their variability is largely modulated by PCP and, consequently, reflecting changes in water residence time in the epikarst.

Further evidence supporting the change in water residence time in the epikarst comes from the $\delta^{234}U_0$ measured in the stalagmite (Table SP1 and Fig. 2C). High $\delta^{234}U_0$ values are usually interpreted to result from dry periods where water–rock interaction time is long, while lower $\delta^{234}U_0$ values can result from wet periods with short water residence time in the epikarst (e.g. Polyak et al., 2012). Under this light, the gradual decrease in $\delta^{234}U$ in BTV21a, from ~3200‰ during the early Holocene to ~2680‰ in the late Holocene indicate a gradual change in the water residence time that is also consistent with the interpretation of the Sr/Ca record.

Fig. 4C shows that Sr/Ca and Ba/Ca in BTV21a are also strongly correlated with calcite $\delta^{18}O$, with Sr/Ca–$\delta^{18}O$ correlation coefficient $R = 0.8794$ and Ba/Ca–$\delta^{18}O$ $R = 0.7726$. Speleothem $\delta^{18}O$ values from Botuverá Cave reflect rainfall $\delta^{18}O$ values (Cruz et al., 2006b, 2005b; Wang et al., 2006, 2007), which is mainly modulated by the pathways that air masses follow before reaching Botuverá (Fig. 1), with more negative $\delta^{18}O$ values for Amazonian moisture during the active phase of the South American Monsoon ($\delta^{18}O \sim 7.0$‰), and rainfall associated with heavier moisture in $^{18}O$ from adjacent Atlantic Ocean when extratropical cyclones ($\delta^{18}O \sim 3.0$‰), reach the coastal area of southern Brazil during the southern hemisphere winter (Cruz et al., 2005b). Combined, the trace element and $\delta^{18}O$ records from BTV21a are a unique archive of SAMS dynamics and changes in mean rainfall in southeastern Brazil throughout most of the Holocene, thus the forthcoming discussions and interpretations will be based solely on the observed variability of Sr/Ca and $\delta^{18}O$.

## 4. Discussion

### 4.1. Millennial scale hydroclimate variability in Botuverá

The combined $\delta^{18}O$ and Sr/Ca ratio records from BTV21a and its strong positive correlation (Fig. 5A) suggests that most of the changes in total rainfall during the Holocene have been driven

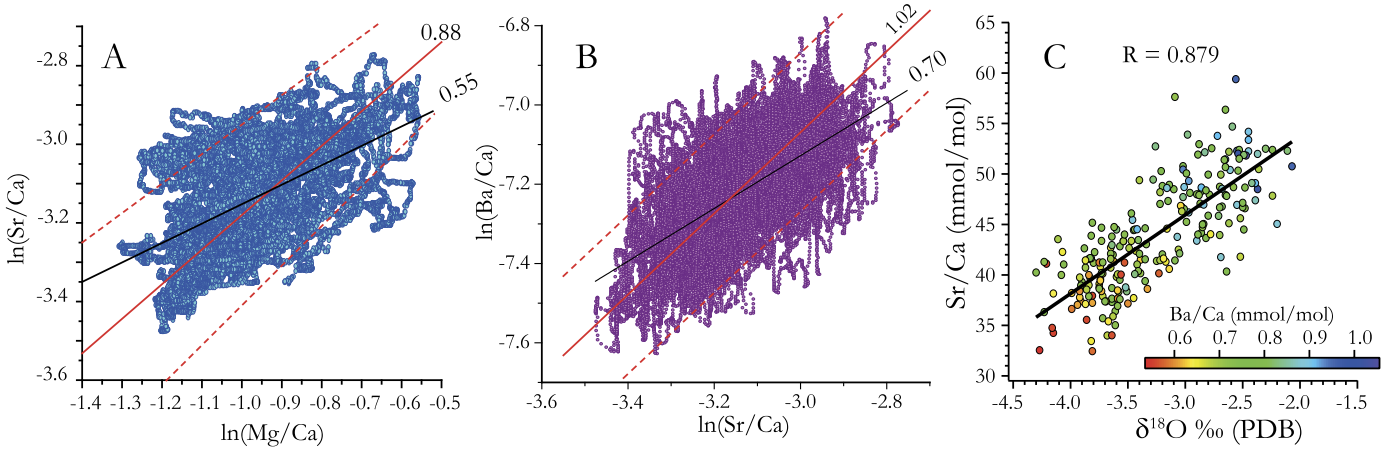


**Fig. 4.** A) Covariation of ln(Mg/Ca) vs. ln(Sr/Ca) showing that the covariance between the molar ratios is mostly affected by PCP, but other processes might be also playing a significant role in the observed variability, in particular Mg/Ca. Black line shows the corresponding linear regression, red line shows the expected slope (solid = 0.88) and their proposed limits (dashed lines) from thermodynamic and kinetic calculation if only PCP is modulating the observed variability (Sinclair, 2011). B) Covariation of the ln(Sr/Ca) vs. ln(Ba/Ca) mol/mol; black and red lines are similar as in A, theoretical lines calculated following the systematics of Sinclair (2011), and the distribution coefficients from Day and Henderson (2013) at 25 °C. Similarity in trends between the theoretical and observed covariation suggests that the hydrological processes affecting Mg/Ca variability did not affect significantly the Sr/Ca and Ba/Ca records, and that the observed variability in these is modulated mostly by PCP. C) Covariance of Sr/Ca with calcite $\delta^{18}O$, symbol color represents the corresponding Ba/Ca for each point and shows that Ba/Ca is also correlated with calcite $\delta^{8}O$ with lower Ba/Ca values (red) clustered at the lower left corner, while high Ba/Ca values (dark blue) clustered at the upper right (reader is referred to the electronic version of the manuscript). (For interpretation of the references to color in this figure legend, the reader is referred to the web version of this article.)

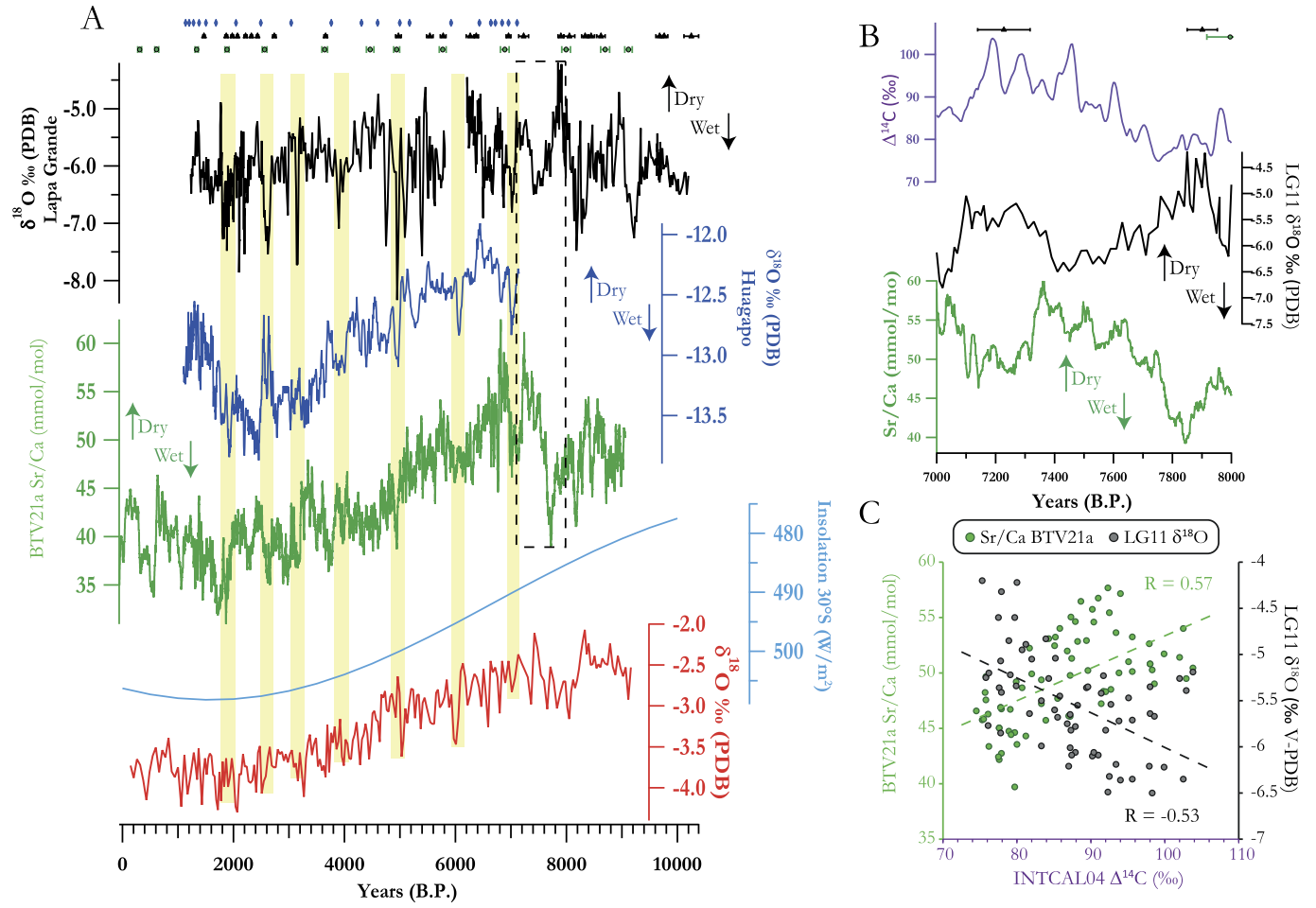


**Fig. 5.** A) Comparison of the Sr/Ca and $\delta^{18}O$ records from BTV21 with the $\delta^{18}O$ record from Lapa-Grande cave (Stríkis et al., 2011) and Huagapo cave (Kanner et al., 2013) showing a correlation between the wet excursions in central eastern Brazil and Amazonia with wet periods in south eastern Brazil. Markers on top show dated points for BTV21a (green) LG (black) and Huagapo (blue). Light blue line is February insolation at 30°S (Berger and Loutre, 1991), note the inverse scale. B) Comparison of LG $\delta^{18}O$ and BTV21a Sr/Ca vs. INTCAL04 (Reimer et al., 2004) $\Delta^{14}C$ for the 7–8 kyr (B.P.) period. C) correlation (anticorrelation) between BTV21a (LG-11) and $\Delta^{14}C$ from INTCAL04. (For interpretation of the references to color in this figure legend, the reader is referred to the web version of this article.)

by SAMS intensity and, thus, it has been the dominant rainfall regime in southeastern Brazil during the last 9000 yr. Moreover, the combined record from BTV21a closely follows summer insolation at 30°S (Fig. 5A), indicating that insolation has not only been the driver for changes in rainfall regimes (tropical vs extratropical) in southeastern Brazil (Cruz et al., 2005a), but also of rainfall amount during the Holocene. The gradual decrease in $\delta^{18}O$ and Sr/Ca and since ~7000 ka indicates an intensification of SAMS from early to late Holocene that resulted in higher mean regional rainfall amount, which reached its long-term optimum 4000 yr ago, when summer insolation changed to its high-phase in the Southern Hemisphere (Figs. 3 and 5). This feature is consistent with previous work by Cruz et al. (2007), and is in accordance with Monsoon precipitation records from Amazon region after 4 kyr that support the enhancement of moisture transport to southeastern Brazil from distal sources (Cheng et al., 2013b).

Our record indicates a suppressed monsoon intensity during the early Holocene, which is consistent with the lower sedimentation rates observed in La Plata Drainage Basin during this period (Razik et al., 2013). This implies that the mean annual rainfall contribution from Amazonian sources into southeastern Brazil was not as important during the early Holocene as it is today. The combined record also suggests that during the early Holocene, with a depressed SAMS (average calcite $\delta^{18}O = -2.5 \pm 0.1‰$), rainfall amount was highly variable but, on average, similar to that observed during the mid-Holocene (5000–6000 yr), when the contribution from Amazonian moisture sources was more significant and resulted in slightly lower average calcite $\delta^{18}O$ ($-3.0 \pm 0.2‰$). Furthermore, our data suggests that during the late Holocene, the total amount of rainfall was higher when compared to the early and mid-Holocene, though its variability was smaller. Such long-term enhancement of SAMS during the Late Holocene is the response to higher austral summer insolation (Fig. 5) and also to a more southern location of the ITCZ during this period (Haug et al., 2001).

The Sr/Ca record from BTV21a shows a series of decadal to centennial-scale excursions towards more humid conditions, some of which are also present in the $\delta^{18}O$ record, suggesting that these represent an enhancement of monsoonal conditions in southeastern Brazil. Fig. 5A compares the Sr/Ca and $\delta^{18}O$ records from Botuverá Cave with two high-resolution records of monsoon variability from South America: Lapa Grande Cave (LG) located in central-eastern Brazil (Stríkis et al., 2011), and Huagapo Cave (HC) from central Andes in Peru (Kanner et al., 2013). The LG record is characterized by a series of large and abrupt excursions towards more negative $\delta^{18}O$ which have been interpreted to be a consequence of cooling in the North Atlantic SST throughout the Holocene (Stríkis et al., 2011), due to the periodical increase in sea-ice and glacial ice circulating in the surface waters of the North Atlantic (Bond et al., 2001). Such events of abrupt monsoon intensification are also observed in the HC and the BTV21a records (Fig. 5A), particularly, during the mid- and late-Holocene, when Amazonian moisture contributions into total rainfall at our site are more significant than in the early Holocene. The most intense of these events occurs at ~5000 yr B.P., as reflected by a ~2‰ excursion in the $\delta^{18}O$ LG record, and about 0.5 to 0.75‰ in the $\delta^{18}O$ HC and BTV21a records, respectively, and has also been recently reported in the northeastern Peruvian Andes (Bustamante-Rosell et al., in press). We note that this event, in particular, corresponds to the most important change in SST in the north Atlantic during the Holocene, as attested by the variability in % of hematite stained glass in marine cores (Bond et al., 2001).

The correspondence of wet events throughout most of South America indicates a widespread intensification of SAMS as a result from cool SST conditions in the North Atlantic. Similar relationships between precipitation amount in tropical America and North Atlantic SST have been previously reported to occur during the Holocene (Baker et al., 2005). However, the geographical extent of these wet periods is unprecedented for South America during the Holocene, and are likely to be the result from the expansion of the geographical extent of the South American Convergence Zone (SACZ), leading to an increase in rainfall amount in most of the South American sub-continent. We note that similar expansion of SACZ has been recently detected to occur during glacial times, also contemporaneous to low North Atlantic SST stadials (Stríkis et al., 2015). The periodic strengthening of SAMS observed here is probably the result from the adjustment of the ITCZ latitude forced by changes in SST in the North Atlantic, resulting in enhanced moisture transport towards western Amazon and, eventually, southeastern Brazil.

The comparison between BTV21a and HC and LG records reveal that monsoon strength in the western Amazon, southeastern and central Brazil have been directly correlated at different stages of the Holocene, however this has not always been the case. This is best exemplified during the 7–8 kyr period where BTV21a and LG records show a remarkable anti-correlation, $R = -0.73$, (Fig. 5B) that is not observed elsewhere in the record comparison. During this period, the Sr/Ca record in BTV21a shows two events when precipitation increased significantly, nearly reaching late-Holocene levels, and centered at 7.8 and 7.2 kyr, respectively, (Figs. 5A–5B). These are accompanied by a slight decrease in $\delta^{18}O$ (~0.5‰), indicating an increase in the proportion of Amazonian moisture reaching southeastern Brazil. Such excursions are mirrored in the LG record by two contemporaneous shifts of up to 1‰ towards less negative $\delta^{18}O$, indicating significant suppressions of the monsoon in central eastern Brazil (Figs. 5A–5B). Such anti-phasing between both sites is likely to be the result from the multidecadal to centennial-scale oscillatory North-South migration of the SACZ leading to wet conditions in Botuverá, and diminished rainfall to the north at Lapa Grande cave site when SACZ shifts to the south. Figs. 5B and 5C compare the BTV21a Sr/Ca record and the $\delta^{18}O$ from LG with the excess of $^{14}C$ in corals and tree rings form INTCAL04 (Reimer et al., 2004) as a proxy of solar irradiance for the 7–8 kyr period, and shows that rainfall amount in southeastern Brazil was tightly correlated with solar irradiance ($R = 0.57$), but anti-correlated in Lapa Grande ($R = -0.53$). Such (anti)correlation between both records and the solar radiation indicates that the SACZ position, hence hydroclimate in southeastern and central Brazil, was non-linearly influenced by solar activity during this period, after which additional forcing factor(s) took over, essentially decoupling precipitation in both places.

### 4.2. Spectral and wavelet analyses

We performed spectral and wavelet analyses of the Sr/Ca record from BTV21a. To simplify the calculation requirements, an annually-resolved time series was generated by resampling from the high-resolution record; we note that de-trending of the dataset did not produce significantly different results as it only eliminated the modes with longer frequencies. Fig. 6A shows the Lomb-Scargle spectrum of the Sr/Ca record obtained using REDFIT (Schulz and Mudelsee, 2002), and it shows a series of signals above the 99% $\chi^2$ red-noise level that attest to the complexity of SAMS and its various modes of oscillation during the Holocene. Fig. 6B shows the Morlet wavelet for modes of oscillation between 256 and 16 yr, and shows that most of the signals above the red-noise level in the Lomb-Scargle spectrum have been quasi-persistent throughout the Holocene, but none of them has been fully persistent during the entire period of stalagmite growth.

The strongest signal above the 99% $\chi^2$ red-noise level in the spectral analysis is centered at 0.013 and 0.018 $yr^{-1}$ (75–55 yr), which is identical to the pattern of oscillatory changes in SST in the North Atlantic (Schlesinger and Ramankutty, 1994), also stated

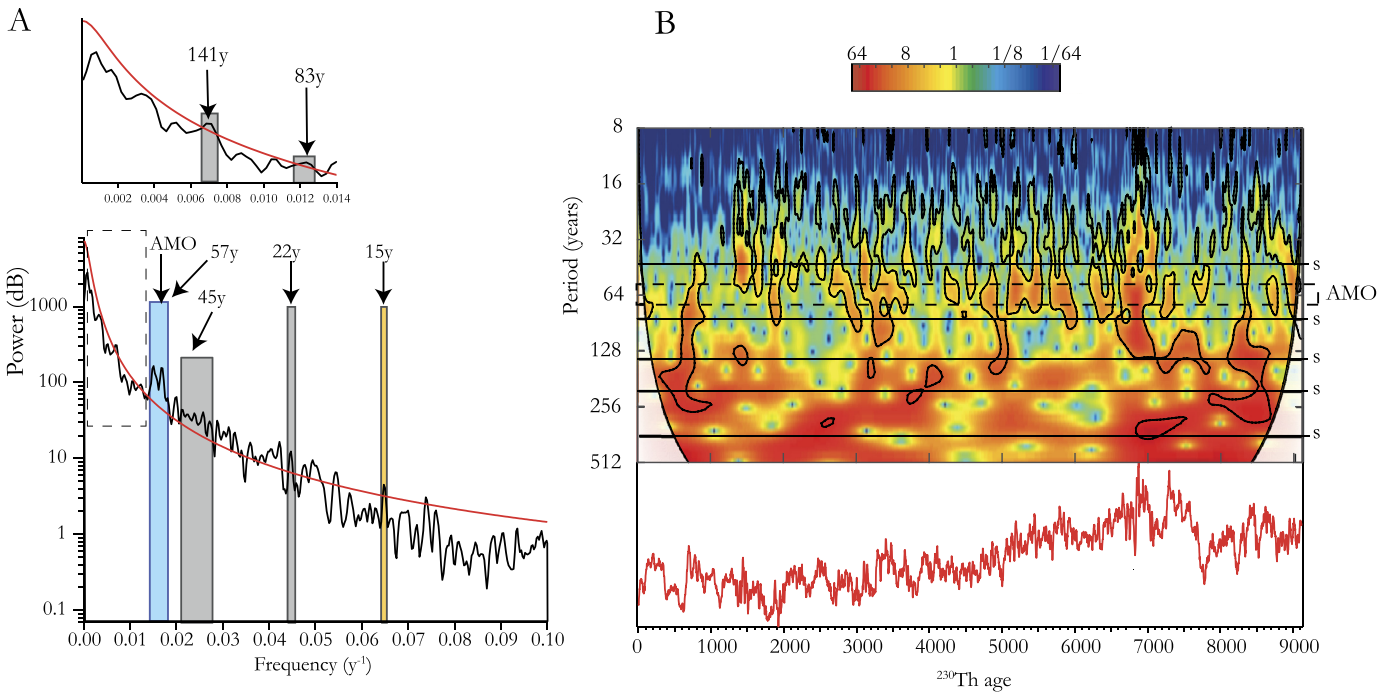


**Fig. 6.** A) Spectral analysis of the Sr/Ca BTV21a record and the $\chi^2$ 99% red-noise level as calculated by Red-Fit (Schulz and Mudelsee, 2002), color bands identify the most prominent oscillations: solar (grey), Atlantic Multidecadal Oscillation (cyan). Inset shows detail of the low-frequency section of the power-spectra. B) Wavelet power spectrum using a Morlet wave function for the Sr/Ca record; shaded areas denote the zone cone of confidence. Dashed box delimits AMO period. Continuous horizontal lines denote solar oscillations. (For interpretation of the references to color in this figure legend, the reader is referred to the web version of this article.)

as the Atlantic Multidecadal Oscillation (AMO). Because the AMO 60-year signal is the strongest in the spectrum, it would appear reasonable to assume that the AMO modulation upon SAMS has been persistent throughout the duration of our record (>9000 yr); however, wavelet analysis of the record (Fig. 6B) shows that the strength of AMO modulation of SAMS has been intermittent throughout the Holocene, with some short periods where very weak or no modulation is detected.

The sporadic strengthening and weakening of AMO modulation has also been observed in several locations in South America, (Apaéstegui et al., 2014a; Bird et al., 2011; Chiessi et al., 2009; Novello et al., 2012; Vuille et al., 2012) as well as in multiple proxies in the Atlantic Basin (Knudsen et al., 2011). Despite this, it is difficult to ascertain the specific role that AMO might have upon SAMS; this is because the periods where the power of the AMO signal is significant are not necessarily associated with strengthening or weakening of SAMS in southeastern Brazil or elsewhere. Moreover, SAMS-AMO coupling is not easily recognized in the reanalysis of modern climate datasets (Garreaud et al., 2009) hampering the use of modern climate dynamics to draw analogue paleoclimatic scenarios.

The spectral analysis also reveals a series of signals above the 99% $\chi^2$ red-noise level corresponding to 141, 85, 67, 57, and 45 yr, which are identical to the periodicity observed for solar cycles detected on variations in atmospheric $^{14}C$ variability recorded in tree-rings (Stuiver and Braziunas, 1989). This indicates that, in addition to the millennial scale solar forcing that has been known to modulate SAMS for over 100 kyr (Cruz et al., 2005a; Wang et al., 2006), and which had an impact on modulating precipitation in Botuverá during the early Holocene (Fig. 6), high-frequency centennial and decadal scale solar oscillations might have also modulated the intensity of the SAMS in southeastern Brazil. Wavelet analysis of the record (Fig. 6B) shows that, similarly as the AMO, modulation by these high-frequency oscillations has not been persistent throughout the Holocene. In contrast, the wavelet analysis also reveals two signals at approximately 420 and 210 yr, those have been persistent throughout the record and were not above the 99% $\chi^2$ red-noise level in the spectral analysis. These also correspond to solar oscillations that were previously detected in the $^{14}C$ record (Stuiver and Braziunas, 1989) and were recently shown to modulate SAMS intensity during the late Holocene (Novello et al., 2012). The results presented here demonstrate that such modulation was persistent during most of the Holocene.

The spectral analysis also reveals the presence of several high-frequency (<50-yr) oscillations above the 99% $\chi^2$ red-noise level. These are complex to interpret since, in contrast to those discussed above, these are not discrete signals, and might be the result of several processes. For example, a 0.045 $yr^{-1}$ signal might correspond to the 22-yr solar cycle, also known as Hale-cycle, (Attolini et al., 1990), whilst high-frequency oscillation modes at 0.055 and 0.072 $yr^{-1}$, corresponding to a 14 and 18 yr, can be interpreted as the effect from the interdecadal oscillation of ENSO (Mann and Park, 1994), which has been recently described as the bi-decadal component of the Pacific Decadal Oscillation (Steinman et al., 2015). Also, a signal at approximately ~0.066 $yr^{-1}$ can be attributed to the interdecadal variability of SACZ at 15 yr (Robertson and Mechoso, 2000). Moreover, considering that extratropical moisture represents a non-negligible fraction of total rainfall in southeastern Brazil (Cruz et al., 2005b), cyclic modulation by the Southern Annular Mode cannot be ruled out as it has been observed in southwestern South America (Mundo et al., 2012), and other reconstructions of SAM index from instrumental data (Visbeck, 2009). From the wavelet analysis, none of these oscillations appears to be persistent throughout the Holocene, with only sporadic periods of high-significance, and most are notoriously absent during the last 1500 yr. However, the presence of these oscillations in the spectral analysis and wavelet analysis attests to the numerous atmospheric and oceanic processes modulating the decadal to centennial variability of SAMS, and highlights the complexity of its interactions.

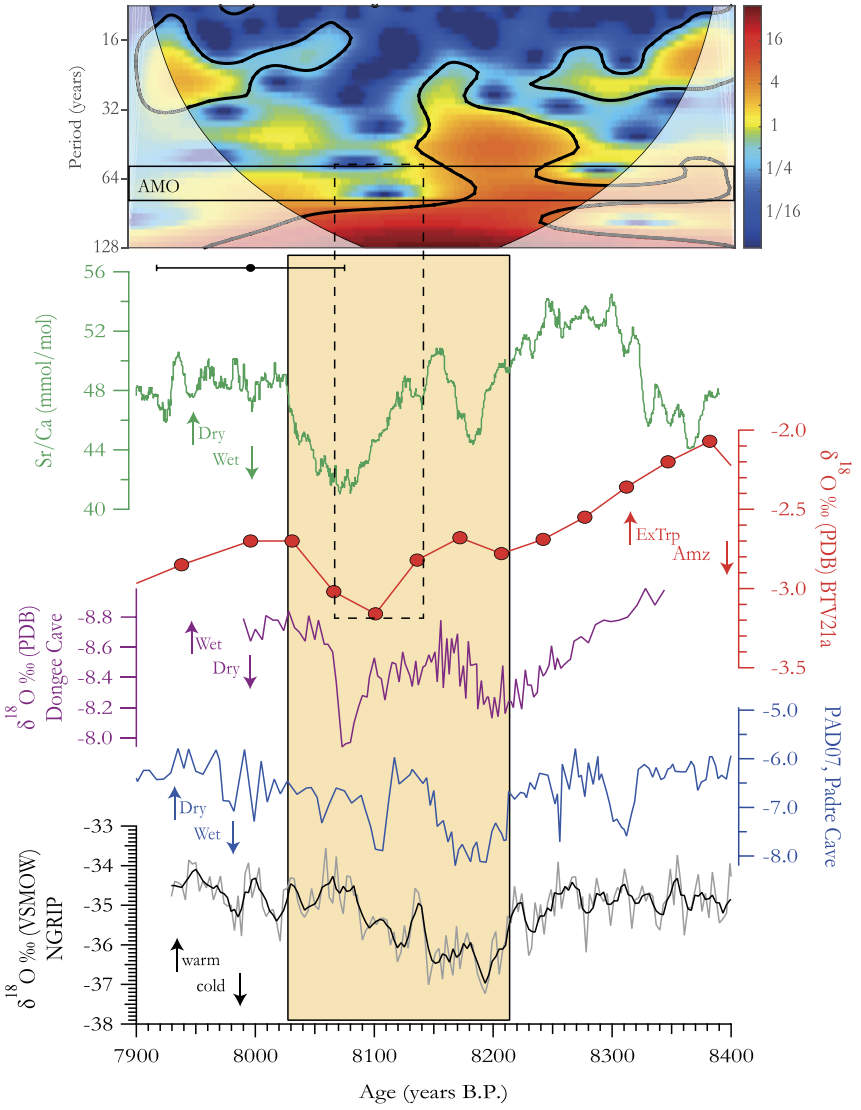


**Fig. 7.** Comparison of the $\delta^{18}O$ and Sr/Ca from BTV21a records for the period between 7.9 and 8.4 ka with the $\delta^{18}O$ records from Padre caves, central Brazil, and Dongee Cave, China (Cheng et al., 2009) and Greenland Ice Core $\delta^{18}O$ composite (Thomas et al., 2007), and the wavelet power spectrum of the Sr/Ca record using Morlet wave function. Shaded areas indicate the cone of confidence and the black lines de 95% confidence intervals. (For interpretation of the colors in this figure, the reader is referred to the web version of this article.)

### *4.3. The expression of Holocene climate anomalies in southeastern Brazil*

#### *4.3.1. The 8.2 event*

Besides the investigation of the long-term hydrological changes at Botuverá cave, our high resolution record allows to study the spatial extent of Holocene climatic events that are well preserved in other climate archives: the 8.2 ka event, the Medieval Climate Anomaly (MCA) and the Little Ice Age (LIA). The 8.2 ka event is the largest global climatic anomaly during the Holocene (Alley et al., 1997), with significant climatic consequences throughout most the Northern Hemisphere (Wiersma and Renssen, 2006) where colder and drier conditions prevailed for nearly 200 yr (Cheng et al., 2009; Thomas et al., 2007) and a southward migration of the average position of the ITCZ (Broccoli et al., 2006) resulted in a weaker monsoon in the north American tropics (Lachniet et al., 2004). Despite the widespread consequences in the Northern Hemisphere, there are only a few records in the Southern Hemisphere (Cheng et al., 2009; Ljung et al., 2008; Sallun et al., 2012), mostly due to the lack of well-dated high-resolution records that allow to resolve multidecadal to centennial abrupt events during the Holocene in large areas over the continent.

Fig. 7 shows the Sr/Ca, and $\delta^{18}O$ records from BTV21a for the 8400–7900 period, and compares them to those obtained in stalagmites from central Brazil (Cheng et al., 2009), and Dongee Cave, in central China (Wang et al., 2005), as well as the high-resolution composite oxygen isotope record from Greenland (Thomas et al., 2007). The Sr/Ca record indicate that during the 8.2 ka event conditions in southeastern Brazil were wetter for about 170 yr, whilst the contemporaneous decrease in the $\delta^{18}O$ record from the very same speleothem suggests that this was the result from an increased proportion of Amazonian precipitation. This finding is in agreement with other proxy records from southeastern Brazil (Sallun et al., 2012), speleothem records from central Brazil (Cheng et al., 2009; Stríkis et al., 2011) indicating an enhancement of SAMS contemporaneous to the event, and in accordance with previous observation that cooling of the North Atlantic results in a monsoon enhancement in both flanks of the SACZ over Brazil. Furthermore, the proxy data are underpinned by model simulations indicating increased precipitation for the duration of this event as a result from the southward migration of the ITCZ (e.g. Broccoli et al., 2006; Morrill et al., 2013).

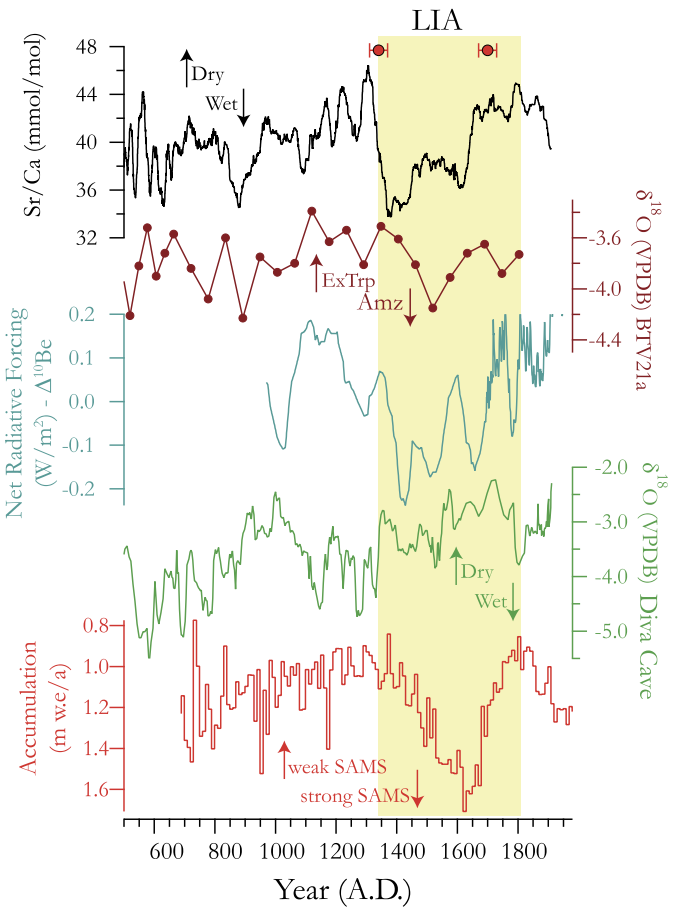


**Fig. 8.** Comparison of the $\delta^{18}$O and Sr/Ca from BTV21a records for the last millennium and compared with the Net Radiative Forcing reconstructed from variability in $^{10}$Be from the Antarctica (Bard et al., 2007), and $\delta^{18}$O records from Diva Cave, northeastern Brazil (Novello et al., 2012) and the Net Balance Accumulation (in meters per year water equivalent), an indicator or regional precipitation estimated for the Quelccaya Ice core (Thompson et al., 2013). Note the reversed axis for the Net Accumulation in the Quelccaya Ice core.

The BTV21a Sr/Ca record replicates the "double-plunge" structure previously detected in Greenland ice-cores (Thomas et al., 2007), stalagmites from Brazil, Oman, and China (Cheng et al., 2009), marine cores from the north Atlantic (Ellison et al., 2006), and suggested by some "hosing" experiments (LeGrande and Schmidt, 2008), providing further evidence on the structure of the event: two distinct cooling events with widespread consequences in both Hemispheres. Wavelet analysis of the annually resolved Sr/Ca record for the "double-plunge" period, 8.4–7.9 kyr B.P. (Fig. 7) shows that the 60–70 yr signal, previously interpreted to reflect the influence of the Atlantic Multidecadal Oscillation (AMO) upon SAMS, is significantly weaker for a period of ~40 yr between 8.05 and 8.1 ka B.P, and particularly during the first half of the second "plunge". This suggest that SAMS was decoupled from AMO modulation and implies that either AMO was severely weakened during the event, or the ocean–atmosphere teleconnections behind the "normal" AMO-SAMS coupling were somewhat interrupted. Weakening of AMO probably resulted in the slowing of AMOC during the event (Ellison et al., 2006). However, because AMO modulation of SAMS has been intermittent throughout the Holocene (Fig. 8B) it is difficult to associate the weakening of AMO modulation ~8100 yr ago solely to the cooling and freshening of the North Atlantic. Although disruption of AMO has been previously suggested as a consequence of the 8.2 ka event (Hillaire-Marcel et al., 2007), no previous record of such disruption is yet available. Moreover, relevant so-called "hosing" experiments (Broccoli et al., 2006; LeGrande et al., 2006; Morrill et al., 2013) are yet to provide detailed information on the periodic ocean–atmosphere interactions (such as AMO) during anomalous paleoceanografic conditions.

#### 4.3.2. The last millennium

Climate during the last thousand years is characterized by two main climatic events: the Medieval Warm Period, also known as Medieval Climate Anomaly, MCA, between ~950 A.D. and 1250 A.D., and the Little Ice Age, LIA, between 1400 A.D. and 1850 A.D. (Mann et al., 2009). Whilst the effects of the MCA are more subtle and not easily distinguishable in many records outside Europe, those from the LIA are more evident at lower latitudes and the tropics (Bird et al., 2011). In South America, the climatic consequences of the LIA are spatially complex (Thompson et al., 2013), and it has been suggested that a dry/wet dipole was formed between Southeastern and Northeasthern Brazil (Novello et al., 2012; Vuille et al., 2012).

Fig. 8 shows the Sr/Ca and $\delta^{18}$O records from BTV21a for the 1500 yr and compares them against the net solar radiative forcing reconstructed from $^{10}$Be abundance in ice cores from Antarctica (Bard et al., 2007), records of rainfall variability of northeastern Brazil from Diva Cave (Novello et al., 2012), and glacier net accumulation from the Quelccaya glacier, eastern Peru (Thompson et al., 2013), an indicator of western Amazonian regional precipitation. The trace element record from BTV21a shows that the increased solar forcing associated with the MCA did not necessarily result in significantly drier conditions in southeastern Brazil. In contrast, the Sr/Ca record in BTV21a indicates that the abrupt decrease in solar forcing at ~1350 A.D. is associated with a contemporaneous enhancement of SAMS, and a gradual increase of Amazonian rainfall throughout the LIA, as suggested by the ~0.5‰ shift in the $\delta^{18}$O record. This is consistent with the gradual increment in water equivalent accumulation observed in the Quelccaya glacier from eastern Peru (Thompson et al., 2013), but also with speleothem records form Cascayunga Cave that suggests increased convective activity over western Amazonia during the Little Ice Age (Reuter et al., 2009), which resulted in enhanced subsidence, hence reduced rainfall, over northeastern Brazil (Novello et al., 2012). Consequently, our record provides evidence to support that the dry/wet dipole observed in orbital timescales between Northeastern Brazil and Botuverá (Cruz et al., 2009), previously suggested only by the Cascayunga Cave record (Novello et al., 2012), was also in place during the Little Ice Age. However, further detailed U–Th dating of the stalagmite is needed to provide a more robust chronological to fundament the climate interpretations at the time interval corresponding to the last millennia in the Botuverá trace-element record, and then to access more definitive answers on the potential climatic consequences of the MCA upon southeastern Brazil and the dynamics of the atmosphere during such relevant event.

## 5. Conclusions

We have shown that the long high-resolution trace element record obtained by LA-ICPMS from stalagmite BTV21a provides a wealth of information on the hydroclimate dynamics of South America for most of the Holocene. This, however, requires prior examination on the geochemical processes occurring in the karst, upstream the stalagmite, which might be modulating the trace element variability in the stalagmite to identify the elements whose variability is most likely to be controlled by Prior Calcite Precipitation. While these processes appear to be common within the Botuverá karst (Cruz et al., 2007; Tremaine and Froelich, 2013), they should not be extrapolated to other localities without thorough assessment.

Our Sr/Ca record indicates that SAMS modulation by the Atlantic Multidecadal Oscillation has been intermittent for most of the Holocene, and in conjunction with other marine (Chiessi et al., 2009) and speleothem (Novello et al., 2012; Vuille et al., 2012) records, it is possible to establish that such modulation/coupling has been in place throughout most of the last 18 ka. Other factors modulating SAMS intensity, include solar oscillation and ENSO, although the effect from the latter is rather subtle.

Because of the complexity in the interpretation of $\delta^{18}O$ variability due to the different moisture sources affecting southeastern Brazil, the trace element record from BTV21a allows to couple the information of SAMS intensity with moisture sources, providing a more robust paleoclimate reconstruction. This allows us to detect complex atmospheric dynamics occurring throughout the Holocene and establish that several forcing factors have modulated the strength of SAMS. Our results suggest the placement of a mega-SACZ during cold stadials in the North Atlantic, similar to those occurring under glacial conditions (Stríkis et al., 2015), yet, the low resolution of contemporaneous hydroclimate records from western Amazonia inhibits full confirmation of such conditions.

The trace element record also provides valuable insights on the climate dynamics during the 8.2 ka event and the Little Ice Age. Our results suggest that the well-known double-plunge structure of the event detected in marine and continental records can be further expanded to southeastern Brazil. However, detailed analysis of our record suggests that the SAMS/AMO coupling that has been in place for most of the last 18 ka, was briefly interrupted for a period of ~100 yr, during the 8.2 ka event. This reveals previously undetected consequences of the abrupt discharge of freshwater into the North Atlantic, and should be verified with further analyses of high-resolution records as well as models of ocean–atmosphere interaction to pinpoint the most likely mechanism. Similarly, the effects of the LIA over southeastern Brazil can also be extracted from our record, and in conjunction with other high-resolution hydroclimate records from South America, we are able to confirm the establishment of the dry/wet dipole between northeastern Brazil, western Amazonia, central Andes and southeastern Brazil.

## Acknowledgements

The authors wish to thank two anonymous reviewers and Dr. Heather Stoll that provided insightful comments on an earlier version of this manuscript. Funding for this project was provided by UNAM/PAPIIT project IN105713 and CONACyT 78828 to JPB, from NASA/FAPESP through the Dimensions of Biodiversity Program Grants 2012/50260-6 and 2013/5029-7 and PRIMO cooperative program (CNPq 590172/2011-5) to FWC, Singapore NRFF2011-08 to XW, and NSF Grant 1103403 to RLE and HC.

## Appendix A. Supplementary material

Supplementary material related to this article can be found online at http://dx.doi.org/10.1016/j.epsl.2016.06.008.

## References

Alley, R.B., Mayewski, P.A., Sowers, T., Stuiver, M., Taylor, K.C., Clark, P.U., 1997. Holocene climatic instability: a prominent, widespread event 8200 yr ago. Geology, 483–486.

Apaéstegui, J., Cruz, F.W., Sifeddine, A., Vuille, M., Espinoza, J.C., Guyot, J.L., Khodri, M., Strikis, N., Santos, R.V., Cheng, H., Edwards, L., Carvalho, E., Santini, W., 2014a. Hydroclimate variability of the northwestern Amazon Basin near the Andean foothills of Peru related to the South American Monsoon System during the last 1600 years. Clim. Past 10, 1967–1981.

Apaéstegui, J., Cruz, F.W., Sifeddine, A., Vuille, M., Espinoza, J.C., Guyot, J.L., Khodri, M., Strikis, N., Santos, R.V., Cheng, H., Edwards, L., Carvalho, E., Santini, W., 2014b. Hydroclimate variability of the northwestern Amazon Basin near the Andean foothills of Peru related to the South American Monsoon System during the last 1600 years. Clim. Past 10, 1967–1981.

Attolini, M.R., Cecchini, S., Galli, M., Nanni, T., 1990. On the persistence of the 22 y solar cycle. Sol. Phys. 125, 389–398.

Auler, A., 2002. Karst areas in Brazil and the potential for major caves – an overview. Bol. Soc. Venez. Espeleol. 36, 29–35.

Baker, P.A., Fritz, S.C., Garland, J., Ekdahl, E., 2005. Holocene hydrologic variation at Lake Titicaca, Bolivia/Peru, and its relationship to North Atlantic climate variation. J. Quat. Sci. 20, 655–662.

Bard, E., Raisbeck, G.M., Yiou, F., Jouzel, J., 2007. Comment on "Solar activity during the last 1000 yr inferred from radionuclide records" by Muscheler et al. Quat. Sci. Rev. 26, 2301–2304.

Basei, M.A.S., Campos Neto, M.C., Castro, N.A., Nutman, A.P., Wemmer, K., Yamamoto, M.T., Hueck, M., Osako, L., Siga, O., Passarelli, C.R., 2011. Tectonic evolution of the Brusque Group, Dom Feliciano belt, Santa Catarina, Southern Brazil. J. South Am. Earth Sci. 32, 324–350.

Berger, A., Loutre, M.F., 1991. Insolation values for the climate of the last 10 million years. Quat. Sci. Rev. 10, 297–317.

Bird, B.W., Abbott, M.B., Vuille, M., Rodbell, D.T., Stansell, N.D., Rosenmeier, M.F., 2011. A 2,300-year-long annually resolved record of the South American summer monsoon from the Peruvian Andes. Proc. Natl. Acad. Sci. 108, 8583–8588.

Bond, G., Kromer, B., Beer, J., Muscheler, R., Evans, M.N., Showers, W., Hoffmann, S., Lotti-Bond, R., Hajdas, I., Bonani, G., 2001. Persistent solar influence on North Atlantic climate during the Holocene. Science 294, 2130–2136.

Borsato, A., Frisia, S., Fairchild, I.J., Somogyi, A., Susini, J., 2007. Trace element distribution in annual stalagmite laminae mapped by micrometer-resolution X-ray fluorescence: implications for incorporation of environmentally significant species. Geochim. Cosmochim. Acta 71, 1494–1512.

Broccoli, A.J., Dahl, K.A., Stouffer, R.J., 2006. Response of the ITCZ to Northern Hemisphere cooling. Geophys. Res. Lett. 33, L01702.

Bustamante-Rosell, M.G., Cruz, F.W., Siffedine, A., Cheng, H., Apaéstegui, J., Vuille, M., Strikis, N., Moquet, J.S., Novello, V.F., Guyot, J., Edwards, L., in press. Holocene changes in Monsoon precipitation in the Andes of NE Peru based on $\delta^{18}O$ speleothem records. Quat. Sci. Rev. http://dx.doi.org/10.1016/j.quascirev.2016.05.023.

Carnaval, A.C., Hickerson, M.J., Haddad, C.F.B., Rodrigues, M.T., Moritz, C., 2009. Stability predicts genetic diversity in the Brazilian Atlantic forest hotspot. Science 323, 785–789.

Cheng, H., Fleitmann, D., Edwards, R.L., Wang, X., Cruz, F.W., Auler, A.S., Mangini, A., Wang, Y., Kong, X., Burns, S.J., Matter, A., 2009. Timing and structure of the 8.2 kyr B.P. event inferred from $\delta^{18}O$ records of stalagmites from China, Oman and Brazil. Geology 37, 1007–1010.

Cheng, H., Lawrence Edwards, R., Shen, C.-C., Polyak, V.J., Asmerom, Y., Woodhead, J., Hellstrom, J., Wang, Y., Kong, X., Spötl, C., Wang, X., Calvin Jr., Alexander E., 2013a. Improvements in $^{230}Th$ dating, $^{230}Th$ and $^{234}U$ half-life values, and U–Th isotopic measurements by multi-collector inductively coupled plasma mass spectrometry. Earth Planet. Sci. Lett. 371–372, 82–91.

Cheng, H., Sinha, A., Cruz, F.W., Wang, X., Edwards, R.L., d'Horta, F.M., Ribas, C.C., Vuille, M., Stott, L.D., Auler, A.S., 2013b. Climate change patterns in Amazonia and biodiversity. Nat. Commun. 4, 1411.

Chiessi, C.M., Mulitza, S., Pätzold, J., Wefer, G., Marengo, J.A., 2009. Possible impact of the Atlantic Multidecadal Oscillation on the South American summer monsoon. Geophys. Res. Lett. 36.

Cruz Jr., F.W., Burns, S.J., Karmann, I., Sharp, W.D., Vuille, M., Cardoso, A.O., Ferrari, J.A., Dias, P.L.S., Viana, O., 2005a. Insolation-driven changes in atmospheric circulation over the past 116,000 years in subtropical Brazil. Nature 434, 63–66.

Cruz Jr., F.W., Karmann, I., Oduvaldo Jr., V., Burns, S.J., Ferrari, J.A., Vuille, M., Sial, A.N., Moreira, M.Z., 2005b. Stable isotope study of cave percolation waters in subtropical Brazil: implications for paleoclimate inferences from speleothems. Chem. Geol. 220, 245–262.

Cruz Jr., F.W., Burns, S.J., Karmann, I., Sharp, W.D., Vuille, M., 2006a. Reconstruction of regional atmospheric circulation features during the late Pleistocene in subtropical Brazil from oxygen isotope composition of speleothems. Earth Planet. Sci. Lett. 248, 495–507.

Cruz Jr., F.W., Burns, S.J., Karmann, I., Sharp, W.D., Vuille, M., Ferrari, J.A., 2006b. A stalagmite record of changes in atmospheric circulation and soil processes in the Brazilian subtropics during the Late Pleistocene. Quat. Sci. Rev. 25, 2749–2761.

Cruz Jr., F.W., Burns, S.J., Jercinovic, M., Karmann, I., Sharp, W.D., Vuille, M., 2007. Evidence of rainfall variations in Southern Brazil from trace element ratios (Mg/Ca and Sr/Ca) in a Late Pleistocene stalagmite. Geochim. Cosmochim. Acta 71, 2250–2263.

Cruz, F.W., Vuille, M., Burns, S.J., Wang, X., Cheng, H., Werner, M., Edwards, R.L., Karmann, I., Auler, A.S., Nguyen, H., 2009. Orbitally driven east–west antiphasing of South-American precipitation. Nat. Geosci. 2, 210–214.

Day, C.C., Henderson, G.M., 2013. Controls on trace-element partitioning in cave-analogue calcite. Geochim. Cosmochim. Acta 120, 612–627.

Ellison, C.R.W., Chapman, M.R., Hall, I.R., 2006. Surface and deep ocean interactions during the cold climate event 8200 years ago. Science 312, 1929–1932.

Fairchild, I.J., Treble, P.C., 2009. Trace elements in speleothems as recorders of environmental change. Quat. Sci. Rev. 28, 449–468.
Fairchild, I.J., Borsato, A., Tooth, A.F., Frisia, S., Hawkesworth, C.J., Huang, Y., McDermott, F., Spiro, B., 2000. Controls on trace element (Sr–Mg) compositions of carbonate cave waters: implications for speleothem climatic records. Chem. Geol. 166, 255–269.
Garreaud, R.D., Vuille, M., Compagnucci, R., Marengo, J., 2009. Present-day South American climate. Palaeogeogr. Palaeoclimatol. Palaeoecol. 281, 180–195.
Grinsted, A., Moore, J.C., Jevrejeva, S., 2004. Application of the cross wavelet transform and wavelet coherence to geophysical time series. Nonlinear Process. Geophys. 11, 561–566.
Hammer, Ø., Harper, D.A.T., Ryan, P.D., 2001. PAST: paleontological statistics software package for education and data analysis. Palaeontol. Electronica 4.
Haug, G.H., Hughen, K.A., Sigman, D.M., Peterson, L.C., Rohl, U., 2001. Southward migration of the intertropical convergence zone through the Holocene. Science 293, 1304–1308. http://dx.doi.org/10.1126/science.1059725.
Hendy, C.H., 1971. The isotopic geochemistry of speleothems–I. The calculation of the effects of different modes of formation on the isotopic composition of speleothems and their applicability as palaeoclimatic indicators. Geochim. Cosmochim. Acta 35, 801–824.
Hillaire-Marcel, C., de Vernal, A., Piper, D.J.W., 2007. Lake Agassiz Final drainage event in the northwest North Atlantic. Geophys. Res. Lett. 34, L15601.
Kanner, L.C., Burns, S.J., Cheng, H., Edwards, R.L., Vuille, M., 2013. High-resolution variability of the South American summer monsoon over the last seven millennia: insights from a speleothem record from the central Peruvian Andes. Quat. Sci. Rev. 75, 1–10.
Karmann, I., Cruz Jr., F.W., Viana Jr., O., Burns, S.J., 2007. Climate influence on geochemistry parameters of waters from Santana–Pérolas cave system, Brazil. Chem. Geol. 244, 232–247.
Knudsen, M.F., Seidenkrantz, M.-S., Jacobsen, B.H., Kuijpers, A., 2011. Tracking the Atlantic multidecadal oscillation through the last 8,000 years. Nat. Commun. 2, 178.
Lachniet, M.S., 2009. Climatic and environmental controls on speleothem oxygen-isotope values. Quat. Sci. Rev. 28, 412–432.
Lachniet, M.S., Asmerom, Y., Burns, S.J., Patterson, W.P., Polyak, V.J., Seltzer, G.O., 2004. Tropical response to the 8200 yr BP cold event? Speleothem isotopes indicate a weakened early Holocene monsoon in Costa Rica. Geology 32, 957–960.
LeGrande, A.N., Schmidt, G.A., 2008. Ensemble, water isotope–enabled, coupled general circulation modeling insights into the 8.2 ka event. Paleoceanography 23, PA3207.
LeGrande, A.N., Schmidt, G.A., Shindell, D.T., Field, C.V., Miller, R.L., Koch, D.M., Faluvegi, G., Hoffmann, G., 2006. Consistent simulations of multiple proxy responses to an abrupt climate change event. Proc. Natl. Acad. Sci. USA 103, 837–842.
Liebmann, B., Mechoso, C., 2011. The South American Monsoon system. In: Chang, C.-P., et al. (Eds.), The Global Monsoon System: Research and Forecast, 2nd ed. World Scientific Publication Company, p. 608.
Ljung, K., Björck, S., Renssen, H., Hammarlund, D., 2008. South Atlantic island record reveals a South Atlantic response to the 8.2 kyr event. Clim. Past 4, 35–45.
Mann, M.E., Park, J., 1994. Global-scale modes of surface temperature variability on interannual to century timescales. J. Geophys. Res., Atmos. 99, 25819–25833.
Mann, M.E., Zhang, Z., Rutherford, S., Bradley, R.S., Hughes, M.K., Shindell, D., Ammann, C., Faluvegi, G., Ni, F., 2009. Global signatures and dynamical origins of the Little Ice Age and medieval climate anomaly. Science 326, 1256–1260.
McDonough, W.F., Sun, S.S., 1995. The composition of the Earth. Chem. Geol. 120, 223–253.
Morrill, C., LeGrande, A.N., Renssen, H., Bakker, P., Otto-Bliesner, B.L., 2013. Model sensitivity to North Atlantic freshwater forcing at 8.2 ka. Clim. Past 9, 955–968.
Mundo, I.A., Masiokas, M.H., Villalba, R., Morales, M.S., Neukom, R., Le Quesne, C., Urrutia, R.B., Lara, A., 2012. Multi-century tree-ring based reconstruction of the Neuquén River streamflow, northern Patagonia, Argentina. Clim. Past 8, 815–829.
Novello, V.F., Cruz, F.W., Karmann, I., Burns, S.J., Stríkis, N.M., Vuille, M., Cheng, H., Lawrence Edwards, R., Santos, R.V., Frigo, E., Barreto, E.A.S., 2012. Multidecadal climate variability in Brazil's Nordeste during the last 3000 years based on speleothem isotope records. Geophys. Res. Lett. 39, L23706.
Polyak, V.J., Asmerom, Y., Burns, S.J., Lachniet, M.S., 2012. Climatic backdrop to the terminal Pleistocene extinction of North American mammals. Geology 40, 1023–1026.
Razik, S., Chiessi, C.M., Romero, O.E., von Dobeneck, T., 2013. Interaction of the South American Monsoon system and the Southern Westerly wind belt during the last 14 kyr. Palaeogeogr. Palaeoclimatol. Palaeoecol. 374, 28–40.
Reimer, P.J., Baillie, M.G.L., Bard, E., Bayliss, A., Beck, J.W., Bertrand, C.J.H., Blackwell, P.G., Buck, C.E., Burr, G.S., Cutler, K.B., Damon, P.E., Edwards, R.L., Fairbanks, R.G., Friedrich, M., Guilderson, T.P., Hogg, A.G., Hughen, K.A., Kromer, B., McCormac, G., Manning, S., Ramsey, C.B., Reimer, R.W., Remmele, S., Southon, J.R., Stuiver, M., et al., 2004. IntCal04 terrestrial radiocarbon age calibration, 0–26 cal kyr BP. Radiocarbon 46, 1029–1058.
Reuter, J., Stott, L., Khider, D., Sinha, A., Cheng, H., Edwards, R.L., 2009. A new perspective on the hydroclimate variability in northern South America during the Little Ice Age. Geophys. Res. Lett. 36, L21706.
Robertson, A.W., Mechoso, C.R., 2000. Interannual and interdecadal variability of the South Atlantic convergence zone. Mon. Weather Rev. 128, 2947–2957.
Sallun, A.E.M., Sallun Filho, W., Suguio, K., Babinski, M., Gioia, S.M.C.L., Harlow, B.A., Duleba, W., De Oliveira, P.E., Garcia, M.J., Weber, C.Z., Christofoletti, S.R., Santos, C.d.S., Medeiros, V.B.d., Silva, J.B., Santiago-Hussein, M.C., Fernandes, R.S., 2012. Geochemical evidence of the 8.2 ka event and other Holocene environmental changes recorded in paleolagoon sediments, southeastern Brazil. Quat. Res. 77, 31–43.
Schlesinger, M.E., Ramankutty, N., 1994. An oscillation in the global climate system of period 65–70 years. Nature 367, 723–726.
Schulz, M., Mudelsee, M., 2002. REDFIT: estimating red-noise spectra directly from unevenly spaced paleoclimatic time series. Comput. Geosci. 28, 421–426.
Shen, C.-C., Lawrence Edwards, R., Cheng, H., Dorale, J.A., Thomas, R.B., Bradley Moran, S., Weinstein, S.E., Edmonds, H.N., 2002. Uranium and thorium isotopic and concentration measurements by magnetic sector inductively coupled plasma mass spectrometry. Chem. Geol. 185, 165–178.
Sinclair, D.J., 2011. Two mathematical models of Mg and Sr partitioning into solution during incongruent calcite dissolution: implications for dripwater and speleothem studies. Chem. Geol. 283, 119–133.
Smith, C.L., Fairchild, I.J., Spötl, C., Frisia, S., Borsato, A., Moreton, S.G., Wynn, P.M., 2009. Chronology building using objective identification of annual signals in trace element profiles of stalagmites. Quat. Geochronol. 4, 11–21.
Steinman, B.A., Mann, M.E., Miller, S.K., 2015. Atlantic and Pacific multidecadal oscillations and Northern Hemisphere temperatures. Science 347, 988–991.
Stoll, H.M., Müller, W., Prieto, M., 2012. I-STAL, a model for interpretation of Mg/Ca, Sr/Ca and Ba/Ca variations in speleothems and its forward and inverse application on seasonal to millennial scales. Geochem. Geophys. Geosyst. 13, Q09004.
Stríkis, N.M., Cruz, F.W., Cheng, H., Karmann, I., Edwards, R.L., Vuille, M., Wang, X., de Paula, M.S., Novello, V.F., Auler, A.S., 2011. Abrupt variations in South American monsoon rainfall during the Holocene based on a speleothem record from central-eastern Brazil. Geology 39, 1075–1078.
Stríkis, N.M., Chiessi, C.M., Cruz, F.W., Vuille, M., Cheng, H., de Souza Barreto, E.A., Mollenhauer, G., Kasten, S., Karmann, I., Edwards, R.L., Bernal, J.P., Sales, H.d.R., 2015. Timing and structure of Mega-SACZ events during Heinrich Stadial 1. Geophys. Res. Lett. 42, 5477–5484A. http://dx.doi.org/10.1002/2015GL064048.
Stuiver, M., Braziunas, T.F., 1989. Atmospheric $^{14}C$ and century-scale solar oscillations. Nature 338, 405–408.
Thomas, E.R., Wolff, E.W., Mulvaney, R., Steffensen, J.P., Johnsen, S.J., Arrowsmith, C., White, J.W.C., Vaughn, B., Popp, T., 2007. The 8.2 ka event from Greenland ice cores. Quat. Sci. Rev. 26, 70–81.
Thompson, L.G., Mosley-Thompson, E., Davis, M.E., Zagorodnov, V.S., Howat, I.M., Mikhalenko, V.N., Lin, P.-N., 2013. Annually resolved ice core records of tropical climate variability over the past ~1800 years. Science 340, 945–950.
Treble, P., Shelley, J.M.G., Chappell, J., 2003. Comparison of high resolution sub-annual records of trace elements in a modern (1911–1992) speleothem with instrumental climate data from southwest Australia. Earth Planet. Sci. Lett. 216, 141–153.
Treble, P.C., Chappell, J., Shelley, J.M.G., 2005. Complex speleothem growth processes revealed by trace element mapping and scanning electron microscopy of annual layers. Geochim. Cosmochim. Acta 69, 4855–4863.
Treble, P.C., Schmitt, A.K., Edwards, R.L., McKeegan, K.D., Harrison, T.M., Grove, M., Cheng, H., Wang, Y.J., 2007. High resolution Secondary Ionisation Mass Spectrometry (SIMS) $\delta^{18}O$ analyses of Hulu Cave speleothem at the time of Heinrich Event 1. Chem. Geol. 238, 197–212.
Tremaine, D.M., Froelich, P.N., 2013. Speleothem trace element signatures: a hydrologic geochemical study of modern cave dripwaters and farmed calcite. Geochim. Cosmochim. Acta 121, 522–545.
Visbeck, M., 2009. A station-based southern annular mode index from 1884 to 2005. J. Climate 22, 940–950.
Vuille, M., Burns, S.J., Taylor, B.L., Cruz, F.W., Bird, B.W., Abbott, M.B., Kanner, L.C., Cheng, H., Novello, V.F., 2012. A review of the South American monsoon history as recorded in stable isotopic proxies over the past two millennia. Clim. Past 8, 1309–1321.
Wang, X., Auler, A.S., Edwards, R.L., Cheng, H., Ito, E., Solheid, M., 2006. Interhemispheric anti-phasing of rainfall during the last glacial period. Quat. Sci. Rev. 25, 3391–3403.
Wang, X., Auler, A.S., Edwards, R.L., Cheng, H., Ito, E., Wang, Y., Kong, X., Solheid, M., 2007. Millennial-scale precipitation changes in southern Brazil over the past 90,000 years. Geophys. Res. Lett. 34, L23701.
Wang, Y., Cheng, H., Edwards, R.L., He, Y., Kong, X., An, Z., Wu, J., Kelly, M.J., Dykoski, C.A., Li, X., 2005. The Holocene Asian monsoon: links to solar changes and North Atlantic climate. Science 308, 854–857.
Wiersma, A.P., Renssen, H., 2006. Model-data comparison for the 8.2 ka BP event: confirmation of a forcing mechanism by catastrophic drainage of Laurentide Lakes. Quat. Sci. Rev. 25, 63–88.